Nanochem Res 9(2): 162-171, Spring 2024

RESEARCH PAPER

Photodegradation of Bisphenol A Using α-Fe_2O_3 Nanoparticles Synthesized by Sonochemical Assisted

Aliakbar Dehno Khalaji

Department of Chemistry, Faculty of Science, Golestan University, Gorgan, Iran

ARTICLE INFO

Article History:
Received 20 January 2024
Accepted 18 March 2024
Published 15 April 2024

Keywords:
α-Fe_2O_3
Sonochemical-assisted
Bisphenol A
Photocatalytic activity

ABSTRACT

In this work, α Fe_2O_3 nanoparticles were prepared by sonochemical assisted method along with calcination at two different temperatures 500 and 700°C for 3h. The α Fe_2O_3 nanoparticles were characterized by FT IR, XRD, VSM and TEM. All results show that the as prepared α Fe_2O_3 nanoparticles are of high purity with ferromagnetic behavior, uniform distribution, and low agglomeration. In addition, photocatalytic degradation of bisphenol A (BPA) was studied by α Fe_2O_3 nanoparticles at the presence of H_2O_2 as an electron trap. Photocatalytic results indicate that 98% and 90% of BPA with the initial concentration of 25 mg/L in the solution were degraded using 0.02 g α Fe_2O_3 nanoparticles within 330 min under the visible light irradiation.

How to cite this article
Dehno Khalaji A. Photodegradation of Bisphenol A Using α-Fe_2O_3 Nanoparticles Synthesized by Sonochemical Assisted . Nanochem Res, 2024; 9(2):162-171. DOI: 10.22036/ncr.2024.02.008

INTRODUCTION

Water pollution is considered one of the most pressing environmental problems in the world today. Industrial wastewater discharges contain hazardous organic natural and synthetic dyes that are highly soluble, stable, and non-biodegradable, and they cause serious damage to human and biological life forms [1]. Therefore, it is urgent and necessary to design an efficient, simple, low-cost, and eco-friendly technique for the removal of organic dyes from wastewater before their discharge in the environment. Until now, numerous techniques, both physical and chemical, have been developed and used for this purpose [2,3]. However, physical techniques often cannot completely remove organic dyes, proving expensive and potentially resulting in the secondary pollution that requires additional arrangement to remove the byproducts [4]. In recent years, advanced oxidation processes (AOP) have been applied for the complete removal of organic dyes from wastewaters [5-7]. They are based on photocatalytic degradation using different transition metal oxides such as Fe_2O_3, Co_3O_4, TiO_2, ZnO, $MgFe_2O_4$ [8-12] and different Fe_3O_4 nanocomposites [13-17]. Among them, hematite (α-Fe_2O_3) stands out as one the most promising options. It is an environmentally friendly semiconductor (n-type) with narrow band gap (E_g = 2.1 eV) that promotes the utilization of visible light in the degradation process and makes α-Fe_2O_3 a competitive candidate as a visible light photocatalyst [18-22]. Hematite is also valuable due to its low cost, high stability, recyclability [18-22], and chemical stability above a wide pH range [23,24]. For example, three α-Fe_2O_3 nanoparticles with different morphologies were synthesized by Khalaji et al. [25] using chemical precipitation and used as photocatalyst for the degradation of methyl orange under visible light irradiation. Weldegebrieal and Sibhatu [26] biosynthesized α-Fe_2O_3 nanoparticles and investigated their photocatalytic activity for the degradation of methyl orange and methylene blue dyes. Rhombohedral α-Fe_2O_3 nanoparticles has been successfully synthesized using P123 soft template assisted route by Ye et al. [27] for photocatalytic degradation of bisphenol A. Bisphenol A (BPA) {4,4-(propane-2,2-diyl)diphenol} is an environmental hormone and a potential endocrine system disrupting

* Corresponding Author Email: *ad.khalaji@gu.ac.ir*

chemical (EDC); it is implicated in various health issues such as cancer and hereditary diseases, and is an extremely toxic organic compound to aquatic organisms [27]. Photocatalytic degradation is one of the best techniques to selectively degrade BPA from wastewaters [27]. In 2023, Khalaji [28] reported the photodegradation of methyl orange and methylene blue using spherical α-Fe_2O_3 nanoparticles.

Recently, we synthesized and characterized new shapes of Fe_2O_3 and investigated the their photodegradation efficiency towards organic dyes [25,28]. In this work, α-Fe_2O_3 nanoparticles were synthesized using sonochemical-assisted method, characterized by several techniques and their photocatalytic activity was evaluated by performing the photodegradation of bisphenol A (BPA) under the visible light irradiation.

EXPERIMENTAL

Materials and methods

All the materials purchased from the Merck Company were of high purity and used as received without additional purification. FT-IR spectra were gathered by a NICOLET IR200 FT-IR spectrometer. Ultraviolet-visible absorption spectra of BPA dye solution were recorded on SHIMADZU UV-Vis spectrophotometer. The XRD diffraction patterns of α-Fe_2O_3 nanoparticles were recorded using Empyrean powder diffractometer of PANalytical in the 2θ range of 10-80°. The TEM images were obtained on a FEI Tecnai G^2 20 microscope with a LaB_6 cathode. The magnetic properties of samples were recorded by SQUID magnetometer.

Preparation of α-Fe_2O_3 nanoparticles

Pure α-Fe_2O_3 nanoparticles were prepared with the chemical precipitation route. To an aqueous solution of $FeCl_3{\cdot}6H_2O$ (1 mmol) in 50 mL of deoxygenated distilled water under magnetic stirring at 80°C, we added benzoic acid (3 mmol) and the mixture was stirred for 15 min. Then, the aqueous solution of 1 M NH_4OH (50 mL) as the precipitating agent was added drop by drop to maintain a pH value of 11, and the mixture was stirred at 80°C for 6 h. The resulting brown precipitates were filtered, washed with cold water and ethanol for three time, dried in an oven at 80°C, and subsequently calcined at 500°C and 700°C for 3h. Finally, the resulting dark-red precipitates were filtered, washed with cold water and ethanol for three time, dried in an oven at 80°C for 24 h.

Photocatalytic studies

The photocatalytic activity of Fe-500 and Fe-700 nanoparticles was investigated by the degradation of bisphenol A (BPA) dye solution with the initial concentration of 30 mg/L under visible light irradiation. The influence of important parameters such as pH solution, contact time, and initial BPA concentration on the photocatalytic degradation of BPA was studied and discussed. The photodegradation efficiency (%) was calculated using the equation as follow, where C_o is the initial BPA concentration and C_t is BPA concentration at time *t*.

$$\text{Photodegradation (\%)} = \{(C_o - C_t) \times 100\} / C_o \quad (1)$$

RESULTS AND DISCUSSION

FT-IR spectra

FT-IR spectra of the as-synthesized Fe-500 and Fe-700 nanoparticles were recorded at room temperature between 4000 and 400 cm^{-1} and are depicted in Fig. 1. The characteristic strong absorption peaks observed at 445, 530 and 645 cm^{-1} in Fe-500 and at 436 and 575 cm^{-1} in Fe-700 can be attributed to the Fe-O band vibrations [18-23]. Also, a broad absorption peak, observed at 3400 cm^{-1} in Fe-500 and 3460 cm^{-1} in Fe-700, is assigned to the O-H stretching of adsorbed water molecules on the surface of Fe-500 and Fe-700, respectively [29-34]. In addition, the very weak absorption peak concerning the bending vibration of adsorbed water molecules is observed at about 1610 cm^{-1} [31].

XRD patterns

XRD analysis were carried out to determine the structure and the average crystallite sizes of the nanoparticles. The obtained XRD patterns of the as-synthesized Fe-500 and Fe-700 samples are shown in Fig. 2. The diffraction peaks in Fe-500 (Fig. 2a) can be indexed in agreement with the expected rhombohedral (JCPDS card 024-0072) [25,26,30,33,34] and the cubic (JCPDS card 032-0469) [34] phase structure of α-Fe_2O_3 consists of 47.7% rhombohedral and 52.3% cubic phase. On the other hand, Fe-700 (Fig. 2b) is comprised purely of hematite. The insets in Fig. 2a and Fig. 2b confimrm that the most intense peak of the cubic phase completely disappeared in the diffraction pattern of Fe-700. The lattice parameters are summarized in Table 1.

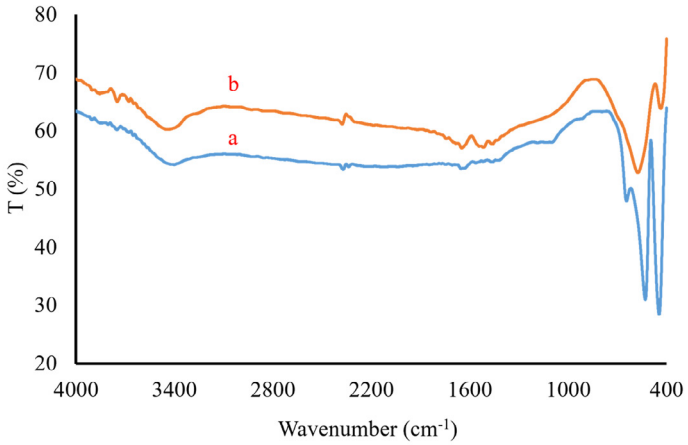

Fig. 1. FTIR spectra of a) Fe500 and b) Fe700

Table. 1. The lattice parameters and average crystallite sizes of Fe-500 and Fe-700

	Fe-500		Fe-700
	Rhombohedral	cubic	rhombohedral
space group	R-3	Ia-3	R-3
a [Å]	5.03258(5)	9.4006(1)	5.02985(9)
c [Å]	13.7419(2)	----	13.7297(4)
phase fraction [%]	47.7	52.3	100
intercept K	0.0714	0.1522	0.0701
crystallite size [nm]	215	101	219

Furthermore, relatively sharp diffraction peaks in both patterns indicate that sizes of the nanoparticles are in the submicron range [29]. The average crystallite sizes were calculated using Williamson-Hall method (Fig. 3), by plotting a graph between β.cosθ and sinθ [24] according to Eq. 2. In this equation, β is FWHM in radians, θ denotes diffraction angle, k is a shape constant between 0.9-1.0, λ represents wavelength of the radiation, D stands for particle size, and ε is strain. Average sizes of crystallites D were determined from the y-intercept of the extrapolated plot:

$$\beta\, cos\theta = \frac{K\lambda}{D} + 4\varepsilon\, sin\theta \quad (2)$$

$$D = k\,.\,\frac{\lambda}{\beta} \quad (3)$$

which gave D = 215 nm for rhombohedral Fe-500, D = 101 nm for rhombohedral Fe-500 and D = 219 nm for rhombohedral Fe-700 (Table 1).

VSM

Magnetic properties of the as-synthesized Fe-500 and Fe-700 nanoparticles were investigated using a vibrating sample magnetometer at 25°C. The magnetization versus applied magnetic field (M-H) curves are displayed in Fig. 4. Both samples exhibited the ferromagnetic behavior [15,18], with maximum M_s of 9.25 emu/g for Fe-500 and 11.36 emu/g for Fe-700. The coercivity (H_c) of samples is ≈ 190 Oe, while the remanent magnetization (M_r) is 2.25 ≈ emu/g for Fe-500 and 2.75 emu/g for Fe-700.The results are in agreement with those reported by Lassoued et al [18] and prove that the magnetic saturation of hematite nanoparticles depends on the structure and particle size [35,36].

TEM

The characterizations of size and morphology were done using TEM analysis and obtained images are shown in Fig. 5. The particle sizes larger than 100 nm can be observed in both TEM images. Besides that, the sample of Fe-500 contains the small-grained fraction, which is in agreement with the results of the Williamson-Hall plot (Fig. 3, Table 1).

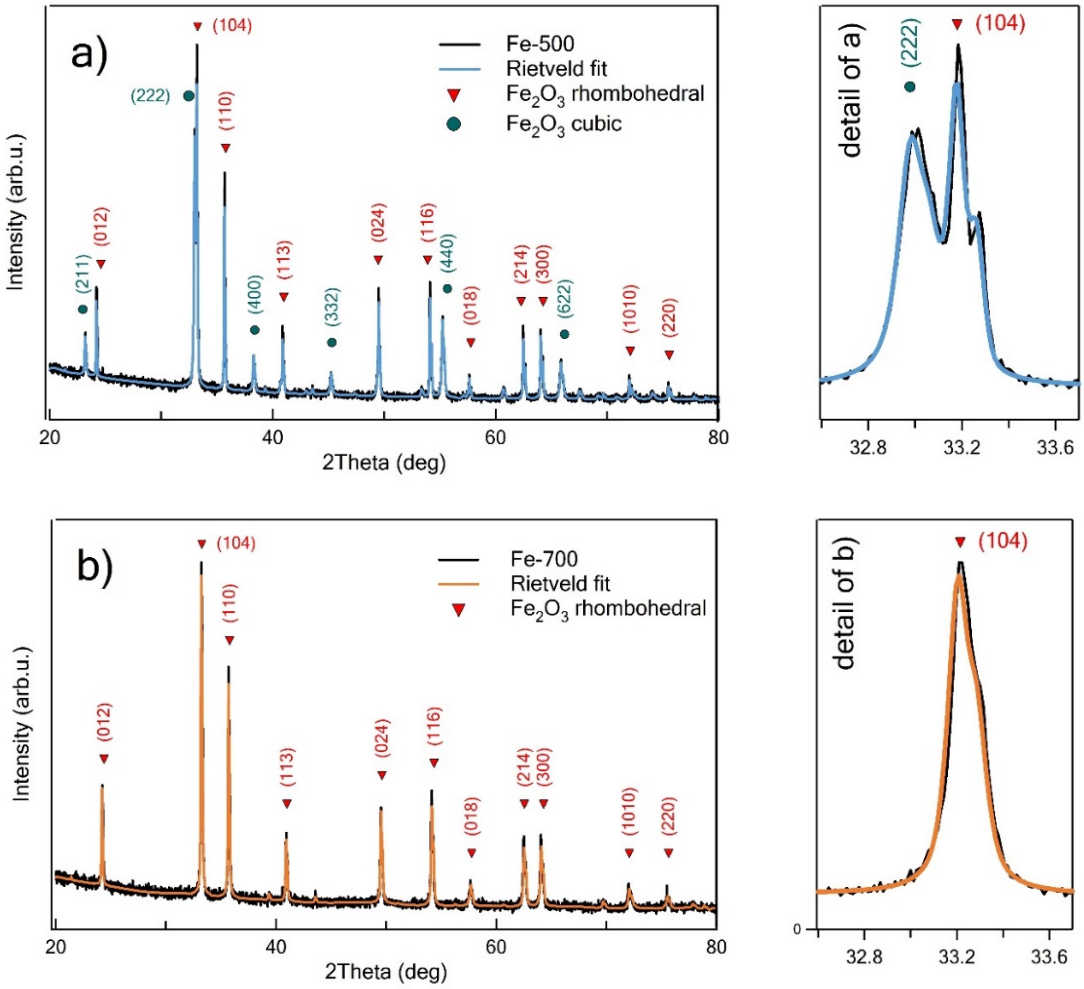

Fig. 2. XRD patterns of a) Fe-500 and b) Fe-700

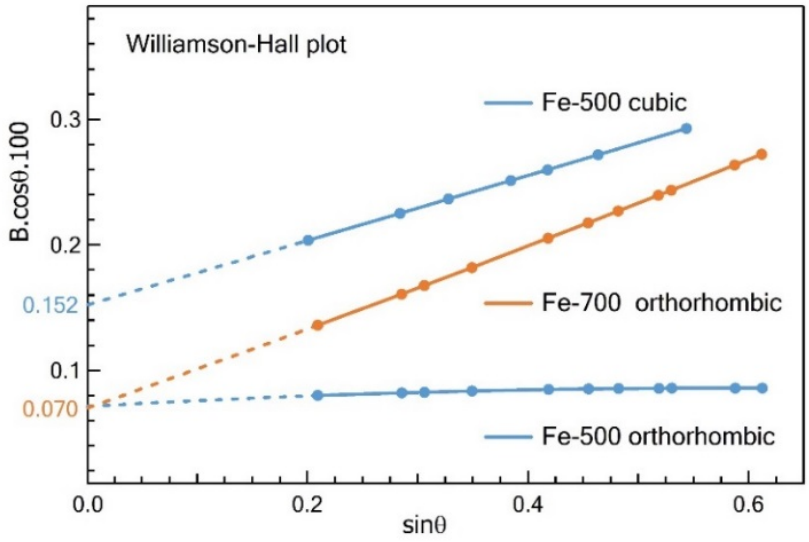

Fig. 3. Williamson-Hall plots of Fe-500 and Fe-700

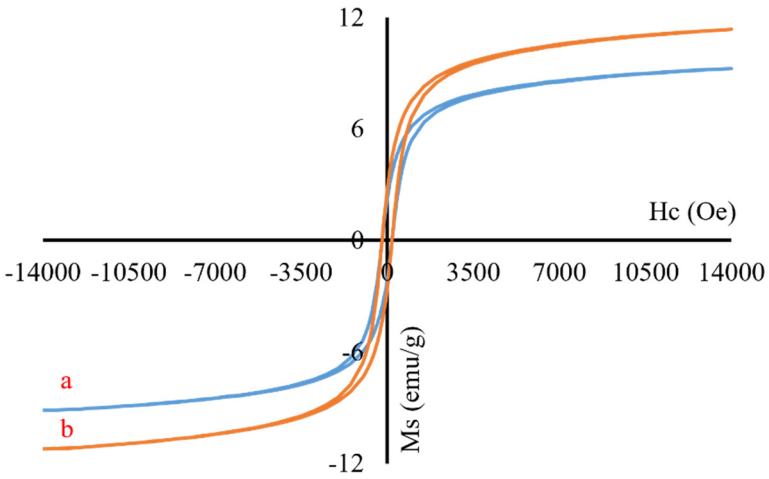

Fig. 4. Magnetic hysteresis loops of a) Fe-500 and b) Fe-700

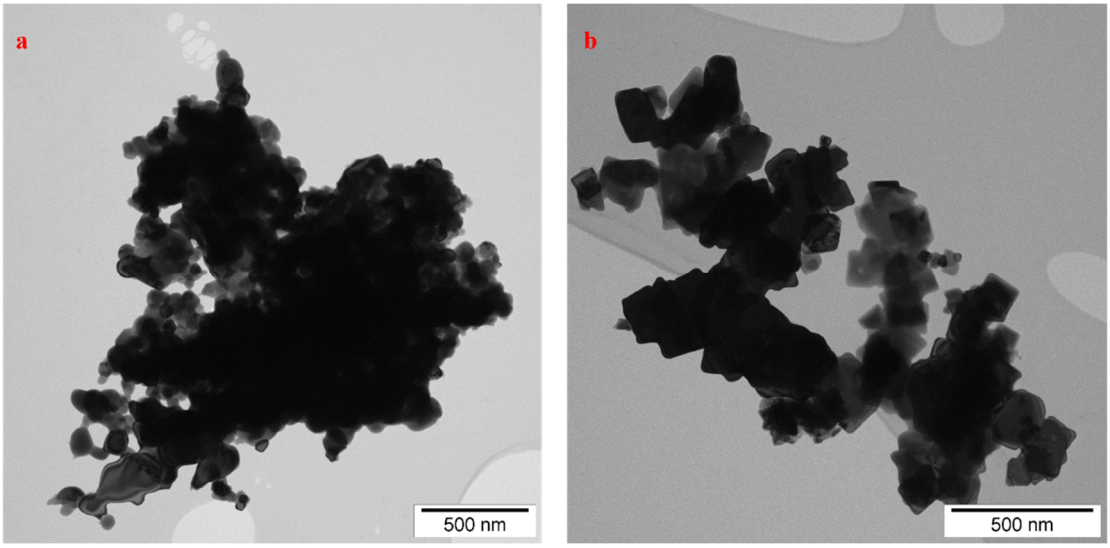

Fig. 5. TEM images of a) Fe-500 and b) Fe-700

Photodegradation of BPA

There are several important parameters for the photocatalytic degradation of organic dyes, such as pH solution, initial BPA concentration, photocatalyst dose and irradiation time [37-43]. The effect of initial pH solution on the photodegradation of BPA using the as-prepared Fe-500 and Fe-700 nanoparticles was studied and the results are shown in Fig. 6.

As shown in Fig. 6, the as-prepared α-Fe_2O_3 nanoparticles had poor photodegradation efficiency at pH of 3, due to the protonation of active groups on the surface of α-Fe_2O_3 nanoparticles as photocatalyst. However, with the increase of pH solution, the surface of α-Fe_2O_3 nanoparticles become deprotonated, creating suitable contact between photocatalyst surface and photogenerated radicals [26]. Therefore, the photocatalytic efficiency increased and reached to the maximum of 98% for Fe-500 and 90% for Fe-700 at the pH solution of 8. Sample Fe-500 exhibited more photocatalytic activity than Fe-600 possibly due to its higher degree of crystallinity [26]. In alkaline pH environment (pH > 8), the electrostatic repulsion between the produced bisphenolate anions and the negatively charged surface of the catalyst prevails and leads to lower photodegradation rates [27]. Further, Fig. 6 indicates that the Fe precursor

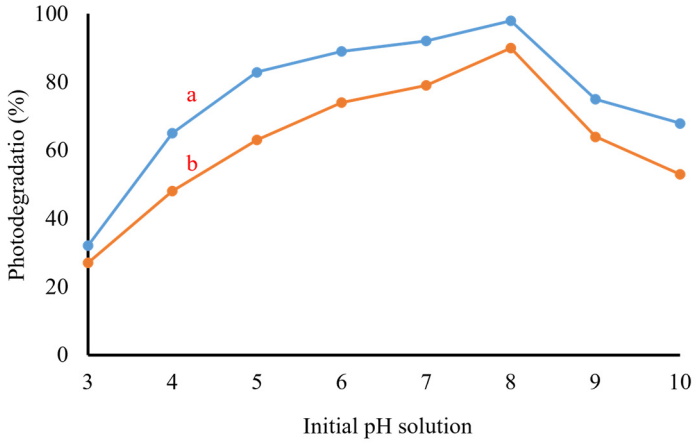

Fig. 6. The effect of initial pH solution on the photodegradation of BPA using a) Fe-500 and b) Fe-700 (30 mg/L, 330 min, 25 °C)

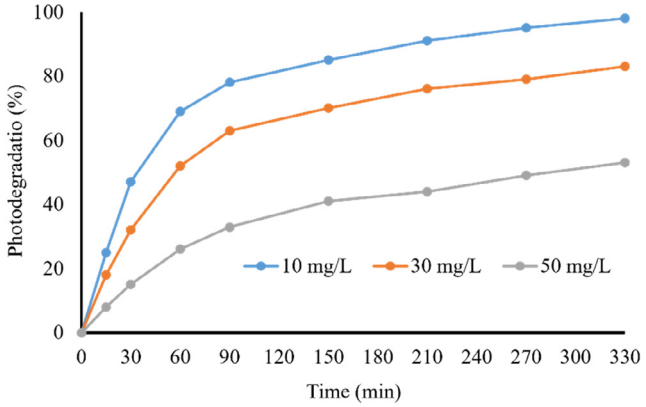

Fig. 7. The effect of initial concentration of BPA and irradiation time on the photodegradation efficiency of Fe-500 (pH 8, 25 °C)

exhibit poor efficiency toward photodegradation of BPA and cannot be used as a photocatalyst.

The effects of the initial BPA concentration and irradiation time on the photodegradation of BPA are demonstrated in Fig. 7 and Fig. 8, respectively. By increasing the initial concentration of BPA from 10 to 30 mg/L, the degradation percentage of BPA was reduced from 98 to 94% for Fe-500 and from 90 to 84% for Fe-700 after 330 min of irradiation due to the limited generation of OH° [19,27] and also lower penetration of photons in the solution phase [19]. From the results it can be concluded that BPA was almost completely adsorbed on the surface of catalysts and only a small amount of BPA molecules remained in the solution. At the initial concentration of BPA of 50 mg/L, the maximum efficiency was 61% for Fe-500 and Fe-700 51% for, indicating that a large amount of BPA remained dissolved and could not be photodegraded. Also, as seen in Fig. 7 and Fig. 8, by increasing the irradiation time, the photodegradation efficiency increased until it reached the saturation level [7,20].

The simplified Langmuir kinetic model [7] was used to evaluate the photocatalytic activity of the as-synthesized Fe-500 and Fe-700 nanoparticles. The plots of $-\ln(C_t/C_o)$ over time are shown in Fig. 9. The linear relationship of the plots confirmed that the photodegradation process follow the pseudo first order kinetic model [4,18-20,25], with the rate constants $k=9.96 \times 10^{-3}$ min^{-1} for Fe-500 and $k=5.55 \times 10^{-3}$ min^{-1} for Fe-700. The calculated data are in agreement with the rate constants reported by Ye et al. [27] and Wang et al [33].

The recyclability and reusability of magnetic materials as photocatalysts or adsorbents is their greatest advantage [19]. The as-synthesized Fe-500 and Fe-700 nanoparticles were recycled by centrifugation, washing twice with distilled water, drying at 75 °C for 3h and then reused for the photodegradation of BPA. Fig. 10 demonstrates

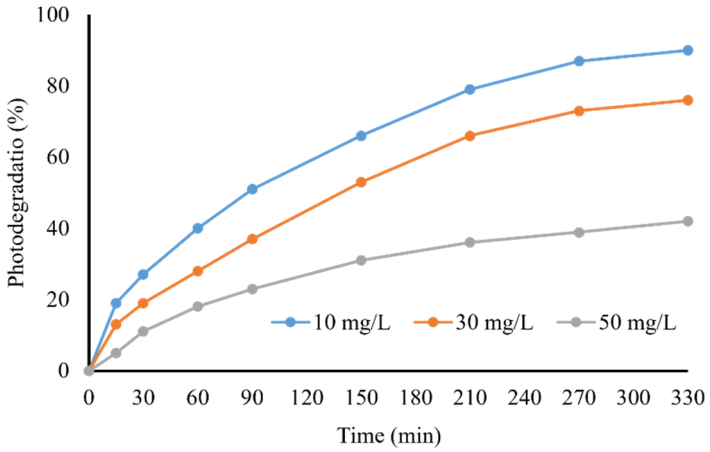

Fig. 8. The effect of initial concentration of BPA and irradiation time on the photodegradation efficiency of Fe-700 (pH 8, 25 °C)

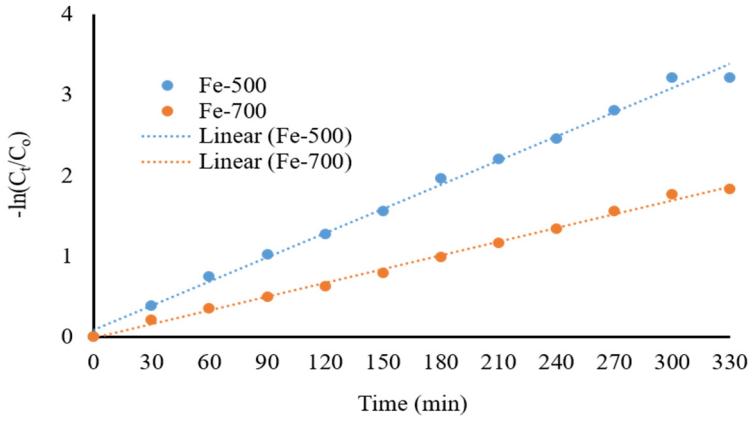

Fig. 9. Pseudo first order kinetic model of the photocatalytic degradation of BPA using as-synthesized Fe-500 and Fe-700 nanoparticles

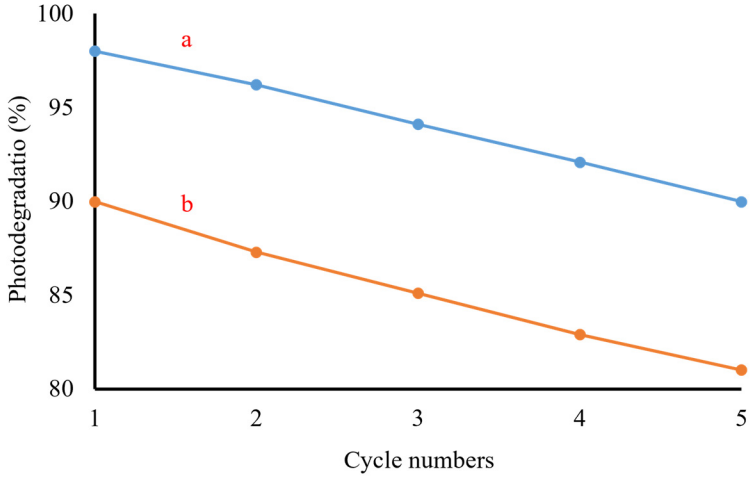

Fig. 10. The effect of cycle numbers of a) Fe-500 and b) Fe-700 on photodegradation of BPA

that the photodegradation of BPA after five cycles was reduced to 90% for Fe-500 and 81% for Fe-700. Small loss of efficiency is due to the deprivation of Fe-500 and Fe-700 nanoparticles during the washing process [9], as well as the obstruction of active sites by adsorbed BPA molecules that were not completely eliminated during washing and dyeing [19,36,40].

The other key factors for the efficiency of photocatalysis are size and morphology of the nanoparticles because there is a direct relationship between specific surface area and number of active sites [18,42]. Further, narrow band gap of the semiconductor promotes absorption of the visible light to produce electron-hole pairs [19,41], which is essential for the photocatalytic process. Upon light irradiation, electrons from the VB can be excited to the CB of the semiconductor, leading to the formation of an electron-hole pair as high oxidative potential to oxidation of organic dyes to reactive intermediates [4-7]. Furthermore, very reactive radicals such as OH° and O_2^{-}° can also be prepared by reaction of electron-hole pair with H_2O and O_2 molecules [4-7].

The possible reaction mechanism of degraded BPA in an equation form is described as follow [19,37,41]:

$Fe_2O_3 + h\nu \rightarrow h^+ + e^-$
$e^- + O_2 \rightarrow O_2^{-}$°
O_2^{-}° $+ H_2O_2 \rightarrow H_2O_2 + OH^- +$ OH°
$e^- + H_2O_2 \rightarrow$ OH° $+ OH^-$
$h^+ + OH^- \rightarrow$ OH°
OH° + BPA → degraded products

Finally, the degraded products of BPA can be deposited on the surface of the as-synthesized Fe-500 and Fe-700 nanoparticles at the bottom of the backer and simply removed by centrifugation of the suspension or by external magnet.

CONCLUSIONS

In summary, two magnetic hematite nanomaterials (Fe-500 and Fe-700) with average diameter sizes of 100-219 nm were successfully synthesized using a simple, and low-cost chemical precipitation route accompanied by calcination at 500 °C and 700 °C. The as-prepared compounds were characterized by several techniques. VSM results confirmed the ferromagnetic behavior of both Fe-500 and Fe-700, known as soft magnetic materials. XRD and TEM results revealed that Fe-700 is pure rhombohedral phase of Fe_2O_3 (hematite) whereas Fe-500 is a mixture of 47.7% rhombohedral and 52.3% cubic phases of Fe_2O_3. In addition, the effect of initial pH solution, BPA concentration and contact time of photodegradation of BPA using as-prepared compounds were studied. The results predicted that the compounds exhibit a high photocatalytic efficiency for BPA (98% for Fe-500 and 90% for Fe-700) in visible light range with a good prospect for their recovery and reusability. Therefore, the as-prepared compounds Fe-500 and Fe-700 will be most promising candidates in wastewater management and removal of different organic dyes.

ACKNOWLEDGMENTS

The author is very grateful for the financial support of Golestan University.

CONFLICT OF INTEREST

The author reports no potential conflict of interest.

REFERENCES

1. Majumder D, Chakraborty I, Mandal K, Roy S. Facet-Dependent Photodegradation of Methylene Blue Using Pristine CeO2 Nanostructures. ACS Omega. 2019;4(2):4243-51.
2. Hammache Z, Soukeur A, Omeiri S, Bellal B, Trari M. Physical and photo-electrochemical properties of MgFe2O4 prepared by sol gel route: application to the photodegradation of methylene blue. Journal of Materials Science: Materials in Electronics. 2019;30(6):5375-82.
3. Salari H, Yaghmaei H. Z-scheme 3D Bi2WO6/MnO2 heterojunction for increased photoinduced charge separation and enhanced photocatalytic activity. Applied Surface Science. 2020;532:147413.
4. Lassoued A, Lassoued MS, Dkhil B, Ammar S, Gadri A. RETRACTED ARTICLE: Photocatalytic degradation of methyl orange dye by NiFe2O4 nanoparticles under visible irradiation: effect of varying the synthesis temperature. Journal of Materials Science: Materials in Electronics. 2018;29(9):7057-67.
5. Lassoued A, Lassoued MS, Dkhil B, Ammar S, Gadri A. Nanocrystalline NixCo(0.5−x)Zn0.5Fe2O4 ferrites: fabrication through co-precipitation route with enhanced structural, magnetic and photo-catalytic activity. Journal of Materials Science: Materials in Electronics. 2018;29(9):7333-44.
6. Elfiad A, Galli F, Djadoun A, Sennour M, Chegrouche S, Meddour-Boukhobza L, et al. Natural α-Fe2O3 as an efficient catalyst for the p-nitrophenol reduction. Materials Science and Engineering: B. 2018;229:126-34.
7. Yang X, Liu Y, Li J, Zhang Y. Effects of calcination temperature on morphology and structure of CeO2 nanofibers and their photocatalytic activity. Materials Letters. 2019;241:76-9.
8. Dehno Khalaji a, Zeinoddin ES, Ghorbani Khorshidi A, Ghaffari A. Visible Light Photodegradation of Methyl

Orange Using α-Fe2O3 Nanoparticles Synthesized via Solvothermal Method in Presence of PVP. Nanochemistry Research. 2023;8(4):278-86.
9. Rekavandi N, Malekzadeh A, Ghiasi E. Methyl orange degradation over nano-LaMnO3 as a green catalyst under the mild conditions. Nanochemistry Research. 2019;4(1):1-10.
10. Taghavi Fardood S, Moradnia F, Mostafaei M, Afshari Z, Faramarzi V, Ganjkhanlu S. Biosynthesis of MgFe2O4 magnetic nanoparticles and its application in photo-degradation of malachite green dye and kinetic study. Nanochemistry Research. 2019;4(1):86-93.
11. Amini M, Ashrafi M. Photocatalytic degradation of some organic dyes under solar light irradiation using TiO2 and ZnO nanoparticles. Nanochemistry Research. 2016;1(1):79-86.
12. Riazian M. Photocatalytic Activity and Nano Structural Investigation on Co3O4 Nanoparticles. Nanochemistry Research. 2020;5(1):46-58.
13. Khodamorady M, Bahrami K. Fe(3)O(4)@BNPs@ZnO-ZnS as a novel, reusable and efficient photocatalyst for dye removal from synthetic and textile wastewaters. Heliyon. 2023;9(6):e16397.
14. Yu R, Shang Y, Zhang X, Liu J, Zhang F, Du X, et al. Self-templated synthesis of core-shell Fe3O4@ZnO@ZIF-8 as an efficient visible-light-driven photocatalyst. Catalysis Communications. 2023;174:106583.
15. Arayesh MA, Kianfar AH, Mohammadnezhad G. Synthesis of Fe3O4/ZrO2/ZnO nanoparticle for enhancing visible light photocatalytic and antibacterial activity. Journal of the Taiwan Institute of Chemical Engineers. 2023;153:105213.
16. Intharaksa O, Nanan S, Patdhanagul N, Panphojan T, Srikakul T, Tantisuwichwong N, et al. Preparation of magnetic CuO/Fe3O4/ZnO photocatalyst for complete degradation of methylene blue under natural sunlight irradiation. Journal of Physics and Chemistry of Solids. 2023;182:111577.
17. Peng Y-D, Ding Y-F, Zheng Y-R, Chai Z-L, Wei Y-X, Wang L, et al. Spectroscopic and theoretical studies on a rare and rigid bis(salamo)-like fluorescent probe for the sequential recognition of Cu2+ and HSO4- ions. Inorganic Chemistry Communications. 2023;158:111598.
18. Kusior A, Michalec K, Jelen P, Radecka M. Shaped Fe2O3 nanoparticles – Synthesis and enhanced photocatalytic degradation towards RhB. Applied Surface Science. 2019;476:342-52.
19. Gupta NK, Ghaffari Y, Bae J, Kim KS. Synthesis of coral-like α-Fe2O3 nanoparticles for dye degradation at neutral pH. Journal of Molecular Liquids. 2020;301:112473.
20. Noruozi A, Nezamzadeh-Ejhieh A. Preparation, characterization, and investigation of the catalytic property of α-Fe2O3-ZnO nanoparticles in the photodegradation and mineralization of methylene blue. Chemical Physics Letters. 2020;752:137587.
21. Silva EdN, Brasileiro ILO, Madeira VS, de Farias BA, Ramalho MLA, Rodríguez-Aguado E, et al. Reusable CuFe2O4–Fe2O3 catalyst synthesis and application for the heterogeneous photo-Fenton degradation of methylene blue in visible light. Journal of Environmental Chemical Engineering. 2020;8(5):104132.
22. Fang J, Xu J, Chen J, Huang X, Wang X. Enhanced photocatalytic activity of molecular imprinted nano α-Fe2O3 by hydrothermal synthesis using methylene blue as structure-directing agent. Colloids and Surfaces A: Physicochemical and Engineering Aspects. 2016;508:124-34.
23. Atabaev TS. Facile hydrothermal synthesis of flower-like hematite microstructure with high photocatalytic properties. Journal of Advanced Ceramics. 2015;4(1):61-4.
24. Zhang Z, Hossain MF, Takahashi T. Self-assembled hematite (α-Fe2O3) nanotube arrays for photoelectrocatalytic degradation of azo dye under simulated solar light irradiation. Applied Catalysis B: Environmental. 2010;95(3):423-9.
25. Khalaji AD, Machek P, Jarosova M. α-Fe2O3 nanoparticles: synthesis, characterization, magnetic properties and photocatalytic degradation of methyl orange. Advanced Journal of Chemistry Section A. 2021;4(4):317-26.
26. Weldegebrieal GK, Sibhatu AK. Photocatalytic activity of biosynthesized α-Fe2O3 nanoparticles for the degradation of methylene blue and methyl orange dyes. Optik. 2021;241:167226.
27. Ye C, Hu K, Niu Z, Lu Y, Zhang L, Yan K. Controllable synthesis of rhombohedral α-Fe2O3 efficient for photocatalytic degradation of bisphenol A. Journal of Water Process Engineering. 2019;27:205-10.
28. Dehno Khalaji A. Spherical α Fe2O3 Nanoparticles: Synthesis and Characterization and Its Photocatalytic Degradation of Methyl Orange and Methylene Blue. Physical Chemistry Research. 2022;10(4):473-83.
29. Lassoued A, Lassoued MS, Dkhil B, Ammar S, Gadri A. Synthesis, photoluminescence and Magnetic properties of iron oxide (α-Fe2O3) nanoparticles through precipitation or hydrothermal methods. Physica E: Low-dimensional Systems and Nanostructures. 2018;101:212-9.
30. Lassoued A, Dkhil B, Gadri A, Ammar S. Control of the shape and size of iron oxide (α-Fe2O3) nanoparticles synthesized through the chemical precipitation method. Results in Physics. 2017;7:3007-15.
31. Lassoued A, Lassoued MS, Dkhil B, Ammar S, Gadri A. Synthesis, structural, morphological, optical and magnetic characterization of iron oxide (α-Fe2O3) nanoparticles by precipitation method: Effect of varying the nature of precursor. Physica E: Low-dimensional Systems and Nanostructures. 2018;97:328-34.
32. Shariatzadeh SMR, Salimi M, Fathinejad H, Hassani Joshaghani A. Nanostructured α-Fe2O3: Solvothermal Synthesis, Characterization, and Effect of Synthesis Parameters on Structural Properties. International Journal of Engineering. 2022;35(6):1186-92.
33. Dehno Khalaji A, Mousavi SM, Palang Sangdevini Z, Jarosova M, Machek P, Dusek M. Hematite (α-Fe2O3) Nanoparticles: Synthesis, Characterization and Optical Properties. Journal of Sciences, Islamic Republic of Iran. 2021;32(3):213-9.
34. Dehno Khalaji A, Palang Sangdevini Z, Mousavi SM, Jarosova M, Machek P. Benzoic acid-functionalized α-Fe2O3 nanoparticles: synthesis, characterization, magnetic and optical properties. Asian Journal of Nanoscience and Materials. 2021;4(2):137-46.
35. Gandha K, Mohapatra J, Hossain MK, Elkins K, Poudyal N, Rajeshwar K, et al. Mesoporous iron oxide nanowires: synthesis, magnetic and photocatalytic properties. RSC Advances. 2016;6(93):90537-46.
36. Qiu M, Wang R, Qi X. Hollow polyhedral α-Fe2O3 prepared by self-assembly and its photocatalytic activities

in degradation of RhB. Journal of the Taiwan Institute of Chemical Engineers. 2019;102:394-402.
37. Araujo RN, Nascimento EP, Firmino HCT, Macedo DA, Neves GA, Morales MA, et al. α-Fe2O3 fibers: An efficient photocatalyst for dye degradation under visible light. Journal of Alloys and Compounds. 2021;882:160683.
38. Liu X, Chen K, Shim J-J, Huang J. Facile synthesis of porous Fe2O3 nanorods and their photocatalytic properties. Journal of Saudi Chemical Society. 2015;19(5):479-84.
39. Jasim SA, Machek P, Abdelbasset WK, Jarosova M, Majdi HS, Khalaji AD. RETRACTED ARTICLE: Solution combustion synthesis of CeO2 nanoparticles for excellent photocatalytic degradation of methylene blue. Applied Physics A. 2022;128(6):475.
40. Saadoon SJ, Jarosova M, Machek P, Kadhim MM, Ali MH, Khalaji AD. Methylene blue photodegradation using as-synthesized CeO2 nanoparticles. Journal of the Chinese Chemical Society. 2022;69(2):280-8.
41. Khurram R, Wang Z, Ehsan MF. α-Fe2O3-based nanocomposites: synthesis, characterization, and photocatalytic response towards wastewater treatment. Environmental Science and Pollution Research. 2021;28(14):17697-711.
42. Hitam CNC, Jalil AA. A review on exploration of Fe2O3 photocatalyst towards degradation of dyes and organic contaminants. Journal of Environmental Management. 2020;258:110050.
43. Wang J, Shao X, Zhang Q, Tian G, Ji X, Bao W. Preparation of mesoporous magnetic Fe2O3 nanoparticle and its application for organic dyes removal. Journal of Molecular Liquids. 2017;248:13-8.